



THE UNIVERSITY *of* EDINBURGH

Edinburgh Research Explorer

Coastal ocean and shelf-sea biogeochemical cycling of trace elements and isotopes: lessons learned from GEOTRACES

Citation for published version:

Charette, MA, Lam, P, Lohan, MC, Young Kwon, E, Hatje, V, Jeandel, C, Shiller, AM, Cutter, GA, Thomas, A, Boyd, PW, Homoky, WB, Milne, A, Thomas, H, Andersson, PS, Porcelli, D, Tanaka, T, Geibert, W, Dehairs, F & Garcia-Orellana, J 2016, 'Coastal ocean and shelf-sea biogeochemical cycling of trace elements and isotopes: lessons learned from GEOTRACES', *Proceedings of the Royal Society A: Mathematical, Physical and Engineering Sciences*. <https://doi.org/10.1098/rsta.2016.0076>

Digital Object Identifier (DOI):

[10.1098/rsta.2016.0076](https://doi.org/10.1098/rsta.2016.0076)

Link:

[Link to publication record in Edinburgh Research Explorer](#)

Document Version:

Peer reviewed version

Published In:

Proceedings of the Royal Society A: Mathematical, Physical and Engineering Sciences

Publisher Rights Statement:

12 month embargo to be set.

General rights

Copyright for the publications made accessible via the Edinburgh Research Explorer is retained by the author(s) and / or other copyright owners and it is a condition of accessing these publications that users recognise and abide by the legal requirements associated with these rights.

Take down policy

The University of Edinburgh has made every reasonable effort to ensure that Edinburgh Research Explorer content complies with UK legislation. If you believe that the public display of this file breaches copyright please contact openaccess@ed.ac.uk providing details, and we will remove access to the work immediately and investigate your claim.



Coastal ocean and shelf-sea biogeochemical cycling of trace elements and isotopes: lessons learned from GEOTRACES

Matthew A. Charette^{*a}, Phoebe J. Lam^b, Maeve C. Lohan^c, Eun Young Kwon^d, Vanessa Hatje^e, Catherine Jeandel^f, Alan M. Shiller^g, Gregory A. Cutter^h, Alex Thomasⁱ, Philip W. Boyd^j, William B. Homoky^k, Angela Milne^l, Helmuth Thomas^m, Per S. Anderssonⁿ, Don Porcelli^o, Takahiro Tanaka^p, Walter Geibert^q, Frank Dehairs^r, Jordi Garcia-Orellana^s

*corresponding author, mcharette@whoi.edu

^aDepartment of Marine Chemistry and Geochemistry, Woods Hole Oceanographic Institution, Woods Hole, MA 02543 USA

^bDepartment of Ocean Sciences, University of California-Santa Cruz, Santa Cruz, CA 95064 USA

^cOcean and Earth Science, National Oceanography Centre, University of Southampton, Southampton SO14 3ZH, United Kingdom

^dResearch Institute of Oceanography, Seoul National University, Seoul 151-742 Korea

^eCentro Interdisciplinar de Energia e Ambiente, Inst. de Química, Universidade Federal da Bahia, Salvador, 40170-115 Brazil

^fLEGOS (CNRS/CNES/IRD/UPS), Observatoire Midi-Pyrénées, Toulouse, 31400, France

^gDepartment of Marine Science, University of Southern Mississippi, Stennis Space Center, MS 39529 USA

^hDepartment of Ocean, Earth, and Atmospheric Sciences, Old Dominion University, Norfolk, VA 23529 USA

ⁱSchool of GeoSciences, University of Edinburgh, Edinburgh, EH9 3FE, United Kingdom

^jInstitute of Marine and Antarctic Studies, University of Tasmania, Hobart, Tasmania, 7005 Australia

^kDepartment of Earth Sciences, University of Oxford, Oxford, OX1 3AN, United Kingdom

^lSchool of Geography, Earth and Environmental Sciences, Plymouth University, Plymouth, PL4 8AA, United Kingdom

^mDepartment of Oceanography, Dalhousie University, Halifax, NS, B3H 4R2 Canada

ⁿDepartment of Geosciences, Swedish Museum of Natural History, Stockholm SE-104 05, Sweden

^oDepartment of Earth Sciences, University of Oxford, Oxford OX1 3AN, United Kingdom

^pAtmosphere and Ocean Research Institute, University of Tokyo
Kashiwanoha 5-1-5 Kashiwa Chiba, 277-8564, Japan

^qMarine Geochemistry Department, Alfred Wegener Institute Helmholtz Centre for Polar and Marine Research, Am Handelshafen 12, 27570 Bremerhaven, Germany

^rEarth System Sciences & Analytical, Environmental and Geo-Chemistry, Vrije Universiteit Brussel, Brussels, B-1050 Belgium

^sPhysics Department-ICTA, Universitat Autònoma de Barcelona, Barcelona, 08193 Spain

Abstract

Continental shelves and shelf seas play a central role in the global carbon cycle. However, their importance with respect to trace element and isotope (TEI) inputs to ocean basins is less well understood. Here, we present major findings on shelf TEI biogeochemistry from the GEOTRACES program as well as a proof-of-concept for a new method to estimate shelf TEI fluxes. The case studies focus on advances in our understanding of TEI cycling in the Arctic, transformations within a major river estuary (Amazon), shelf sediment micronutrient fluxes, and basin-scale estimates of submarine groundwater discharge. The proposed shelf flux tracer is ²²⁸radium ($T_{1/2}=5.75$ y), which is continuously supplied to the shelf from coastal aquifers, sediment porewater exchange, and rivers. Model-derived shelf ²²⁸Ra fluxes are combined with TEI/ ²²⁸Ra ratios to quantify ocean TEI fluxes from the western North Atlantic margin. The results from this new approach agree well with previous estimates for shelf Co, Fe, Mn, and Zn inputs and exceed published estimates of atmospheric deposition by factors of ~3-23. Lastly, recommendations are made for additional GEOTRACES process studies and coastal margin-focused section cruises

that will help refine the model and provide better insight on the mechanisms driving shelf-derived TEI fluxes to the ocean.

1. Introduction

Continental shelves and shelf seas play an important role in modulating the transfer of materials between the land and ocean. As such, quantifying processes occurring within this key interface is essential to our understanding of the biogeochemistry of trace elements and their isotopes (TEIs) in the ocean, a major goal of the GEOTRACES program (www.geotraces.org). Moreover, the supply and removal of elements in coastal oceans have direct influence on the structure of ocean ecosystems and their productivity. Although coastal oceans comprise only around 7% of the total ocean area, they support 15-20% of total primary productivity and provide 90% of the world's fish yield [1]. As a critical Earth system interface, a large proportion of CO₂ exchange between the ocean and atmosphere occurs over the shelf, which is thought to be a net sink for both atmospheric and terrestrial carbon [2-4].

In the nearshore environment, estuaries are known to be important zones of TEI processing [5]. One classic example is the removal of dissolved iron during estuarine mixing, which has been shown in many cases to vastly diminish the riverine flux of this element to the ocean [6-8]. Similarly, uranium has an active biogeochemistry in estuaries and salt marshes, which generally, yet not exclusively, act as sinks for dissolved U [9-11]. Dissolved organic matter (DOM) and several other trace elements may also be removed, at different rates, along the salinity gradient of estuaries and shelves [8, 12-15], while some TEIs like barium and radium are known to be added due to desorption from riverine particles [16-20]. In addition to rivers [21], submarine groundwater discharge (SGD) may represent a large source of TEIs to the coastal ocean [22, 23]. Comprising a mixture of meteoric groundwater and seawater circulated through coastal aquifers, SGD has been estimated to exceed river discharge both regionally [24, 25] and by a factor of 3-4 on a global basis [26]. Furthermore, SGD has been shown to be an important source of micronutrients (e.g.

Fe [27]), contaminants (e.g. Hg [28] and Pb, [29]), and TEIs commonly used as paleo-tracers (e.g. U and Ba [30]).

For some elements, boundary exchange processes involving sedimentary deposits on the continental margins may have substantial or even greater fluxes to the ocean than rivers. Diffusive benthic fluxes can be a major source of dissolved rare earth elements (REE) to the ocean at levels that could explain the missing source observed in recent isotopic modeling studies [31-33], where the REE flux from shelf sediments is larger than other REE sources to the ocean [34]. The sedimentary remobilization of Nd along continental margins, specifically due to sediment dissolution, also illustrates the importance of shelf porewater exchange processes as a source of TEIs to the ocean [31]. Studies at “mid-ocean” shelves, such as the Kerguelen and Crozet Plateaus, showed a substantial role of sedimentary iron release in alleviating Fe limitation and enhancing carbon sequestration in the Southern Ocean [35-37].

The GEOTRACES program has carried out basin scale sections to quantify and identify the processes that supply TEIs at ocean boundaries (atmosphere-ocean, sediment-water, ocean crust-overlying water, continent-ocean [38-41]). However, the coastal or shelf ocean is an interface that requires additional process studies to investigate the key processes impacting on the biogeochemical cycles of TEIs. The identification and quantification of TEI distributions and fluxes along ocean margins are important for a number of reasons, including their sensitivity to changing precipitation and wind patterns, and potential impacts on aquaculture and fisheries. Particularly striking is the extent and rate at which humans have modified the coastal zone worldwide [42], a narrow strip of land within 100 km of the ocean where half of the world’s population lives and where three-quarters of all large cities are located [43, 44]. The impacts are numerous and include large-scale bottom water anoxia, eutrophication, acidification, overfishing and anthropogenic contaminant inputs. For instance, global budgets of TEIs such as Pb and Hg have already been significantly altered in the ocean as a result of human induced

activities such as acid mine drainage [45, 46]. The role of changing sea-ice cover may affect shelf TEI transport rates, and TEI discharges associated with the accelerated melting of large ice sheets have the potential to increase in magnitude over the coming decades to centuries. For present-day Greenland, the Fe flux may already be on par with the total amount of Fe delivered to the North Atlantic Ocean via dust [47], but the scale of this impact depends on the quantification of fluxes between the coast and open ocean [48].

An understanding of the mechanisms governing the linkages between the terrestrial→shelf→open ocean continuum is crucial [49]. Although some GEOTRACES process studies have focused more in near shelf regions, GEOTRACES sections to date have, by design, focused primarily on open ocean transects. Here we highlight several examples of where GEOTRACES studies have yielded significant insight on shelf TEI processes, defined as those occurring along ocean margins at water depths <200 m. We further propose a new approach for quantifying the shelf flux of TEIs using a radium isotope tracer (^{228}Ra) and inverse modeling techniques. Finally, we recommend a series of efforts that are necessary to constrain the exchange processes at coastal/shelf ocean interfaces and to aid in the prediction of fluxes of TEIs from this boundary to the ocean.

2. Significant GEOTRACES contributions to our understanding of shelf impacts on TEI budgets for the open ocean

2.1 The Arctic

The Arctic Ocean is unique among the major ocean basins in having as much as one half of its area taken up by shelves [50]. Further, the basin receives a disproportionate percentage of the world's river discharge (10% [51]). Arctic waters are also highly stratified, with a distinct low salinity surface mixed layer, a strong halocline, and clear shelf and river inputs. Because of these features, the impact of shelf-basin interactions on TEI distributions is particularly prominent throughout the Arctic Ocean. However, TEI data have been limited due to the logistical difficulties of reaching remote and ice-covered regions. The International

Polar Year 2007-2008 provided a launching pad for the GEOTRACES program, with five cruises in the Arctic region between 2006-2009, which led to new insights about important Arctic coastal processes acting on TEI distributions. More recently, in summer 2015 three nations mounted full GEOTRACES Arctic cruises; the results of that coordinated effort are forthcoming.

High concentrations of shelf-derived trace metals in surface waters of the central Arctic were reported by Moore [52]. This included Cd, which has been found to exhibit only minor isotope shifts compared to other ocean basins where greater variations are generated through biological removal [53]. Data from the Swedish-Russian GEOTRACES (GIPY13) cruise to the Siberian shelves found that Cd was not removed in the Lena estuary, and there were further Cd additions to shelf waters from the shelf sediments [54]. Another example of shelf influence on the deep basin is the distribution of Ba, which is strongly enriched in estuarine waters due to desorption from river sediments. In theory, Ba distributions can delineate shelf TEI sources; however, isolating the terrestrial Ba source may be complicated due to biogenic Ba uptake and vertical redistribution [55]. As part of the Canadian IPY-GEOTRACES, a dissolved Ba cross-section through the Canadian Archipelago revealed high surface water Ba concentrations near the Horton River and a pronounced Ba maximum in the upper halocline waters (Fig. 1; [56]). The latter was thought to be due in part to Ba released to subsurface waters in the wake of organic matter remineralization, a finding similar to Roeske et al. [55] who reported that remineralization from the Siberian shelf led to a similar Ba enrichment below the surface mixed layer. This may represent a dynamic process that is not at steady-state: such 'metabolic Ba' concentrations in the subsurface layer increase with the arrival of organic matter sometime after the spring bloom, approaching maximum values toward the end of winter [56].

A strong Mn enrichment was also found in the surface layer of the central basin due to riverine inputs of Mn (Fig. 2; [57]), though the inferred river component indicated that river waters were significantly depleted by estuarine processes. Mid-depth

enrichments of Mn on the shelf also suggested that there were benthic contributions, though this sediment source did not extend a significant distance off-shelf. The first measurements of Ga in Arctic waters found that its distribution reflected mixing between Atlantic and Pacific waters, with evidence of both riverine input and scavenging removal in shelf waters of the Beaufort Sea [58]. Further studies of the shelf cycling of Ga and related elements (especially Al, which is chemically similar to Ga though more readily scavenged) could provide insights into how shelf scavenging removal affects the off-shelf transport of reactive TEIs.

Isotope variations in Nd have been widely used to understand shelf-water interactions and riverine inputs. Within the Arctic Ocean, gradients between surface and halocline waters reflected inputs from the Pacific [59] as well as a source that isotopically matched the major rivers, indicating that the concentrations of the river components reaching the central basin did not reflect the considerable estuarine Nd losses commonly seen elsewhere [60]. These datasets were extended with samples from the BERINGIA 2005 and GIPY13 GEOTRACES cruises, which clearly demonstrated how Nd isotopes and concentrations in the Pacific layer were modified while crossing the Bering Sea through sediment-water exchange processes as was inferred for other shelf areas (Fig. 3; [61]). Furthermore, Lena River waters did not suffer strong modification through estuarine losses like in the Amazon [62].

Data from GEOTRACES cruises have also documented the behavior of carbon on the Arctic shelves. Alling et al. [63] demonstrated for the first time that substantial degradation of DOC occurs in the Lena River estuary, with greater degradation in the broad East Siberian Seas where shelf water residence times are several years; along with degassing of CO₂, this process was clearly shown in DIC $\delta^{13}\text{C}$ signatures [64]. Rising Arctic Ocean temperatures are leading to the thawing of permafrost and release of its stored methane [65, 66]. Indeed, preliminary results from the recent 2015 U.S. GEOTRACES Arctic section (GN01) show shelf enrichments of tracers such as CH₄ [67], though the impact of this process on other TEIs remains to be seen.

Essential to addressing these and other questions, are radioactive TEIs, which allow for quantification of the time scales associated with these shelf-basin exchange processes, as has been demonstrated by Rutgers van der Loeff et al. [68] for ^{228}Ra and more recently by Rutgers van der Loeff et al. [69], who used the $^{228}\text{Th}/^{228}\text{Ra}$ daughter/parent ratio, which is depleted on the shelves but climbs in the particle-depleted central basin, to estimate an age of 3 years for waters at the Gakkel Ridge.

2.2 The influence of major rivers

River-dominated shelves have the potential to be important point sources for TEI delivery to marginal seas and their adjacent ocean basins. For example, Nd isotopic compositions have been measured together with dissolved and colloidal REE concentrations and radium isotope activities in the Amazon estuary salinity gradient as part of the [GEOTRACES process study AMANDES](#) (Fig. 4; [13]). The sharp drop in REE concentrations in the low-salinity region was driven by the coagulation of colloidal material. At mid salinities, dissolved REE concentrations increased, a result of REE release from lithogenic material, a conclusion supported by the Nd isotopic signature within the estuary. Concurrent measurements of the short-lived Ra isotopes (^{223}Ra , $t_{1/2}=11.4$ d and ^{224}Ra , $t_{1/2}=3.7$ d) revealed that this dissolution process is rapid, on the time scale of 3 weeks. These findings have significant implications for the global marine Nd budget and other TEIs that undergo similar sediment-water exchange processes. This study reinforces one of the original concepts of the GEOTRACES program: the power of synoptic and multiple TEI sampling approaches to understanding ocean biogeochemical cycling.

2.3 Evidence for eddy-mediated cross-shelf transport of iron

Although dust deposition is considered the dominant source of iron to the open ocean, it has now been well established that long-range transport of shelf Fe in high nutrient low chlorophyll (HNLC) regions are a factor in the development of blooms 100's to 1000's of kilometers offshore (e.g. [37, 70-72]) and can dominate iron supply on the global scale [73]. While radium isotopes have been used to quantify this source [74-76], isolating the shelf source on basin-scales is not easily

accomplished in regions beyond the Southern Ocean where other inputs (e.g. dust, hydrothermal vents) may be co-occurring. A 2008 GEOTRACES process study, 'FeCycle', focused on biogeochemical cycling within an eddy off the eastern seaboard of the north island of New Zealand, which is seasonally oligotrophic and has spring diatom blooms [77]. The study revealed that the iron supply for these blooms comes from cross shelf transport of metals that are likely 'picked up' on the shelf and moved offshore in an eddy. This conclusion was reached based on high dissolved and particulate Mn within the eddy and from trajectory analysis using a satellite altimetry model (Fig. 5).

2.4 Apportioning sources of iron using iron isotopes

In addition to transport models, isotopes of iron have recently been used as tracers of oceanic Fe sources [78-81]. Novel high throughput methods [82] have enabled high-resolution sampling on ocean section cruises like GEOTRACES. Recently, Conway and John [83] used this approach to apportion iron sources to the North Atlantic according to dust input, hydrothermal venting, and two types of sediment fluxes: reductive and non-reductive sedimentary release. While they estimated that dust was the dominant Fe source, they reported that non-reductive release from sediments on the North American margin was a major local source that contributed between 10-19% of the iron basin-wide (Fig. 6). In addition, Fitzsimmons et al. [84] reported that ~60-80% of the dissolved Fe in this region was in the colloidal phase, which has implications for the bioavailability and long-range transport of this important micronutrient. At the African margin, reductive dissolution in sediments accounted for 1-4% of the iron basin-wide [83]. Further south, Homoky et al. [85] attributed a high-proportion of dissolved Fe present in margin sediments to non-reductive release, and earlier studies of pore waters that were rich in colloidal iron had similar isotope compositions [86, 87], which supports the view that colloids may influence the stability and transport of iron from non-reductive sediment sources in ocean basins [88].

2.5 Time variations in basin-scale submarine groundwater discharge

Submarine groundwater discharge has received increased attention over the past two decades as a source of TEIs to the ocean. The majority of the early studies focused on the local scale, though Moore et al. [24] was able to estimate SGD to the Atlantic Ocean using ^{228}Ra ($T_{1/2}=5.75$ y) inventories from the Transient Tracers in the Ocean (TTO) program, and determined that the SGD flux was $2\text{--}4\times 10^{13}$ m³/y, equivalent to 80-160% of the freshwater discharge from rivers. Since the TTO data had been collected in the 1980s, the Atlantic Ocean ^{228}Ra inventory had largely decayed and been replaced by the time of the 2010-11 U.S. GEOTRACES North Atlantic program. This afforded Charette et al. [89] the opportunity to evaluate whether or not this ocean basin was in steady-state with respect to SGD inputs. Using ^{228}Ra data collected along transects between North America and West Africa, and Western Europe and West Africa, they observed essentially no change in the upper ocean inventory of this tracer, suggesting that SGD had not changed despite significant changes in groundwater withdrawals during the intervening period.

Kwon et al. [26] took this a step further and used inverse modeling techniques applied to a global ^{228}Ra dataset to calculate total SGD to the ocean. This approach yields the total ^{228}Ra flux from the shelf, which in addition to the SGD input includes the riverine discharge and shelf sediment diffusive sources. Sediments of continental shelves and aquifers are important areas for in situ production of Ra isotopes through continuous decay of their parent thorium isotopes (e.g. Moore et al. [90], while rivers supply dissolved Ra isotopes as well as Ra sourced from desorption from suspended sediments in the estuarine mixing zone [91]. For a number of TEIs, estimates for riverine inputs are generally well constrained, however, due to estuarine processing and direct TEI inputs to the shelf we lack a method or approach for quantifying the net flux of TEIs across the interface between coastal and open ocean waters.

2.6 ^{228}Ra as a shelf TEI flux gauge

To this end we are proposing an approach for quantifying shelf TEI fluxes that utilizes ^{228}Ra as a shelf flux gauge. This method takes advantage of the global inverse

model of Kwon et al. [26], which focused on isolating the flux ^{228}Ra via SGD to the ocean, but at its root is designed to estimate the total ^{228}Ra flux from all shelf sources required to balance the upper ocean ^{228}Ra inventory and decay. Because of its strong shelf source and relatively short half life (on the time scale of mixing), the majority of the upper 1000 m ^{228}Ra inventory in the basin can be traced back to the shelf. This inverse approach to estimating shelf ^{228}Ra flux has the advantage of integrating the shelf source of ^{228}Ra over annual to decadal timescales, which averages out seasonal variability that hampers the use of nearshore ^{228}Ra gradients to estimate shelf ^{228}Ra fluxes directly [92]. As a first order estimate, we propose to use the ratio of nearshore gradients of dissolved TEI and ^{228}Ra measured over the shelf and nearby stations during specific GEOTRACES cruises to link the model-derived shelf-ocean ^{228}Ra flux to shelf-ocean TEI fluxes.

The full details of the global ^{228}Ra model can be found in Kwon et al. [26]. Briefly, the model employs a $2^\circ \times 2^\circ$ global circulation model where the domain is restricted to between 60°S and 70°N due to insufficient ^{228}Ra coverage in the polar oceans. The vertical resolution is fine near the surface (~ 40 m) and coarse near the ocean bottom (~ 600 m). The coastal ^{228}Ra source is defined as that originating from the ocean grid boxes adjacent to land boxes with a depth of less than ~ 200 m. The coastal source is optimized through a minimization scheme whereby the reported fluxes are those that result in the best fit between the model and observed ^{228}Ra activities in the basin. The total ^{228}Ra fluxes for each $2^\circ \times 2^\circ$ margin grid cell are shown in Figure 7a. The highest total margin inputs are to the North Pacific and Indian Ocean basins. For both the Atlantic and Pacific Oceans, the western margin ^{228}Ra fluxes exceed those from the east, likely due to a combination of major river inputs, SGD, and the presence of broad continental margins and/or extensive shelf seas. The relatively narrow shelf along the North American active margin in the Pacific appears to have the lowest inputs on average.

Assuming shelf-ocean exchange is primarily driven by eddy diffusion, the net cross-shelf TEI flux can be linearly scaled with the net cross-shelf ^{228}Ra flux as follows:

$$TEI\ flux = {}^{228}Ra\ flux \times \left(\frac{\Delta TEI}{\Delta {}^{228}Ra} \right) = {}^{228}Ra\ flux \times \left(\frac{TEI_{shelf} - TEI_{ocean}}{{}^{228}Ra_{shelf} - {}^{228}Ra_{ocean}} \right) \quad (1)$$

where TEI_{shelf} and ${}^{228}Ra_{shelf}$ are the average concentrations of the TEI of interest and ${}^{228}Ra$ over the shelf water column (<200 m). The TEI_{ocean} and ${}^{228}Ra_{ocean}$ are the average dissolved TEI and ${}^{228}Ra$ in the open ocean (<200 m) (see supplementary material). For highly reactive elements with very low open ocean concentrations, this ratio may be close to $(TEI_{shelf} / {}^{228}Ra_{shelf})$. However, for this approach to be applicable to TEIs with a wide range of particle reactivities, including those with non-negligible open ocean concentrations relative to shelf concentrations, $\Delta TEI / \Delta {}^{228}Ra$ should be employed. For shelves where the net cross-shelf advective flux is substantial, the TEI flux would not scale linearly with ${}^{228}Ra$ flux as illustrated in the supplementary materials.

It is important to recognize that fluxes derived from this approach are the net dissolved TEI input rate to the ocean at the shelf break (200 m). Hence, the flux at this boundary is not necessarily what might be expected to reach the ocean interior due to the varying degrees of TEI particle reactivity and biological cycling. Further, the method in theory should account for any TEI removal over the shelf; therefore, fluxes may not equal the sum of the inputs along the boundary (e.g. rivers, SGD, sediment diffusion). Finally, we note that many of the TEI shelf input and removal processes vary seasonally, not necessarily in concert with seasonal variability in ${}^{228}Ra$ sources, and that not all shelf sources are expected to have uniform $\Delta TEI / \Delta {}^{228}Ra$. For example, sporadic sources due to rivers and SGD may hinder a proper averaging of $\Delta TEI / \Delta {}^{228}Ra$ over large shelf areas. While the spatial and temporal variability in a particular $\Delta TEI / \Delta {}^{228}Ra$ must be fully assessed before this method is to be widely employed, we hope that this exercise provides a first order assessment of the importance of shelf TEI fluxes to the ocean in comparison to other external sources.

For the purpose of this exercise, we chose to focus on the North Atlantic Ocean basin due to the availability of synoptic TEI and ${}^{228}Ra$ data from the U.S. GEOTRACES GA03

cruises, though the scope could be expanded as more GEOTRACES datasets become available. These cruises crossed or approached three main shelf areas: the Northwest Atlantic shelf south of Woods Hole, MA (USA), the Iberian margin, and the Mauritanian upwelling zone off of Western Africa. For perspective, the combined North Atlantic shelf ^{228}Ra flux ($23.9 \pm 4.6 \times 10^{22}$ atoms/y) accounts for approximately 25% of the global shelf flux ($96 \pm 5 \times 10^{22}$ atoms/y; Fig. 7a; [26]). Of the three GA03 cruise shelf crossings, however, only the Northwest Atlantic has multiple stations in close proximity to the shelf break and a shelf where elemental transport is dominated by eddy diffusion [93]. As a result, the western North Atlantic shelves (0° - 70°N), which are responsible for about 60% of the shelf ^{228}Ra input to this ocean basin ($14.3 \pm 1.9 \times 10^{22}$ atoms/y), will be the focus of our shelf TEI flux calculations.

Though there is a long list of TEIs fluxes that could be determined using this method, we chose to focus on four (dissolved Fe, Mn, Co, Zn) that span a range of particle reactivity and play a role in upper ocean biogeochemical cycling. The $\Delta\text{TEI}/\Delta^{228}\text{Ra}$ ratios were calculated using equation (1) from averaged concentration data for the two Northwest Atlantic nearshore stations (GA03, KN204-1 stations 1,2) and open ocean station 16 (GA03, KN204-1; Fig. 7b).

By combining the model ^{228}Ra fluxes and $\Delta\text{TEI}/\Delta^{228}\text{Ra}$, we can estimate the annual shelf TEI inputs to the western North Atlantic Ocean (Table 1). The western N. Atlantic shelf Co flux ($1.4 \pm 0.4 \times 10^8$ mol/y) is consistent with literature estimates from a variety of independent approaches. Saito et al. [94] estimated that the shelf dissolved Co flux for the Peru upwelling region was 2.0×10^7 mol/y, which compares well with our estimate considering that we integrated over a ~ 7 times larger area. Lateral shelf area normalized Co fluxes of 6.2 - $10 \mu\text{mol m}^{-2} \text{y}^{-1}$ were reported by Bown et al. [95] for the S. Atlantic near Cape Town. These are a factor of ~ 5 - 10 lower than the shelf-normalized fluxes for the western N. Atlantic margin (Table 1;

56 $\mu\text{mol m}^{-2} \text{y}^{-1}$), though their estimate was based on transport across a boundary several hundred km from the shelf-break.

The $\Delta\text{TEI}/\Delta^{228}\text{Ra}$ approach yielded a shelf Fe flux of $3.9 \pm 1.4 \times 10^8 \text{ mol/y}$ for the western N. Atlantic. When normalized to shelf-area, this flux is $160 \mu\text{mol m}^{-2} \text{y}^{-1}$. Sedimentary Fe inputs [88], which are expectedly higher as they do not account for any removal over the shelf, range from $900 \mu\text{mol m}^{-2} \text{y}^{-1}$ [73] to $1570 \mu\text{mol m}^{-2} \text{y}^{-1}$ [71] to $2700 \mu\text{mol m}^{-2} \text{y}^{-1}$ [96]. On a global scale, the shelf-sedimentary Fe inputs as reported by Tagliabue et al. [73], Elrod et al. [71], and Dale et al. [96] are $2.7 \times 10^{10} \text{ mol/y}$, $8.9 \times 10^{10} \text{ mol/y}$, and $7.2 \times 10^{10} \text{ mol/y}$, respectively. The western N. Atlantic Ocean total shelf input as determined by our method would therefore represent only 0.4-1.4% of the global sediment flux. If we assume that our $\Delta\text{Fe}/\Delta^{228}\text{Ra}$ is comparable to the global shelf average, our approach would predict a global shelf-ocean Fe flux of $2.3 \times 10^9 \text{ mol/y}$. If the western N. Atlantic shelf is representative of shelf systems globally, our model suggests that only a small fraction of the shelf sedimentary Fe input is exported to the open ocean and therefore available for biological uptake where Fe may be limiting.

The western N. Atlantic Mn shelf flux is $5.4 \pm 1.0 \times 10^8 \text{ mol/y}$ or $220 \mu\text{mol m}^{-2} \text{y}^{-1}$. Literature values for shelf Mn fluxes are largely focused on the shelf sediment source. For example, Landing and Bruland [97] reported sedimentary Mn flux of up to $140 \mu\text{mol m}^{-2} \text{y}^{-1}$ for the Monterey Shelf, while McManus et al. [98] observed much higher values for the Oregon/California shelf ($2900 \pm 900 \mu\text{mol m}^{-2} \text{y}^{-1}$). The former agrees quite well with our estimate based on equation (1) while the latter is likely higher due to the high productivity associated with the strong upwelling in that region. Lastly, the total Zn shelf flux is $1.6 \pm 0.6 \times 10^9 \text{ mol/y}$ or $630 \mu\text{mol m}^{-2} \text{y}^{-1}$. To the best of our knowledge, the shelf Zn flux estimates reported herein are the first of their kind.

In terms of other major sources to the surface ocean, shelf inputs can be on par with or even dominant for certain TEIs. The dissolved cobalt flux for the western N. Atlantic shelf alone is over an order of magnitude higher than the atmospheric deposition of soluble Co to the entire ocean basin as reported by two independent studies ($\sim 11 \times 10^6$ mol/y; [99, 100]). Soluble Fe (wet+dry) atmospheric deposition to the tropical N. Atlantic ranges from $2.9\text{--}43 \mu\text{mol m}^{-2} \text{y}^{-1}$ [101]; scaled to the basin the atmospheric Fe flux becomes $1.2\text{--}18 \times 10^8$ mol/y or 31–460% of the western North Atlantic dissolved shelf flux using the TEI/ ^{228}Ra approach. Powell et al. [101] also reported soluble (wet+dry) atmospheric Mn fluxes, which we scaled to the N. Atlantic ($0.75\text{--}15 \times 10^8$ mol/y), equivalent to 14–280% of the shelf inputs reported herein. Assuming 15% solubility, Little et al. [102] estimated the atmospheric Zn input to the surface ocean to be 6.9×10^7 mol/y; our estimates for the western North Atlantic shelf alone exceed that flux by a factor of ~ 23 . Higher concentrations of Zn along with lighter isotopes were observed at both eastern and western Atlantic margins indicating sediments were a source of Zn to this region [83]. Our net shelf-ocean flux of Zn is almost a factor of three higher than the Little et al. [102] *global* estimate for riverine input (5.9×10^8 mol/y); this is in contrast with their suggestion that scavenging removal of Zn and burial in continental margin sediments might represent the “missing sink” for Zn in the global ocean mass balance for this element.

3. Recommendations for the future

We have presented a possible path forward in quantifying TEI shelf-open ocean exchange rates using ^{228}Ra and demonstrated the potential of the method by focusing on the western North Atlantic Ocean. This exercise was made possible by publication of a recent global model for shelf radium inputs and synoptic TEI and ^{228}Ra measurements on a series of U.S. GEOTRACES cruises in 2010–11. Since Ra isotope measurements are not a requirement for GEOTRACES compliance, we suggest that future section cruises and shelf process studies include at least ^{228}Ra so that we can better understand how to relate this tracer to other TEIs. Ra isotope data are especially needed for the Indian and Pacific Oceans where historical data

coverage is sparse. Shelf process studies would be needed for a range of shelf settings, i.e. how do $\Delta\text{TEI}/\Delta^{228}\text{Ra}$ ratios vary seasonally and as a function of hydrological state, shelf width, and coastline lithology (e.g. karst vs. volcanic)? Lastly, for shelf environments where advection plays an important role in TEI transport, a second conservative tracer in addition to ^{228}Ra would be needed to constrain the shelf-ocean TEI flux (Supplementary Material).

While we have used an inverse approach, which was based on a coarse resolution model, in order to calculate shelf fluxes at a near basin-wide scale, a finer resolution model needs to be combined with coastal ^{228}Ra and TEI data in order to constrain various shelf TEI sources more precisely. Where ^{228}Ra measurements are not possible on future GEOTRACES cruises, we advocate for concurrent physical measurements that may also be used to quantify the shelf flux of TEIs. For example, Tanaka et al. [103] combined DFe distributions with turbulence measurements using a vertical microstructure profiler (VMP) in the Bering Sea; they found that productivity in this region was driven in part by injections of iron-rich subsurface layer at the southeastern shelf break.

Our discussion above highlights the potential importance of shelf processes on open ocean TEI distributions. Results to date are somewhat limited because of the programmatic emphasis placed on open ocean full depth profiles. For example, lack of data over the shelf for GA03 precluded the inclusion of the eastern boundary shelves in our analysis of TEI fluxes to the North Atlantic Ocean. To better understand the role of shelf input to the open ocean (and vice versa) in global TEI budgets, future GEOTRACES sections may need to be reconfigured with an increased emphasis on shelf stations. Given the shallow depths involved, this change would not impact ship-time requirements to any significant extent. Also, sections in regions with wide shelves and high ratios of shelf area to open water will be particularly useful. The recent 2015 Canadian, U.S., and German sections in the Arctic Ocean are examples of this approach. Fortunately, Ra isotopes were measured on all three cruises.

There are a number of margin-centric GEOTRACES sections that have been identified in the program planning documents but have yet to be realized due to a variety of factors. These include two of the three proposed for the coastal China seas, Brazil margin, and the Gulf of Mexico. Regarding the latter, the 2007 GEOTRACES Atlantic Workshop Report identified a section through the Caribbean and Gulf of Mexico that contains significant opportunities to examine shelf impacts. Roughly a third of the area of the Gulf of Mexico is comprised of shelf waters less than 200 m deep. Portions of the coastline are river dominated (Mississippi) while others are groundwater runoff dominated carbonate platforms (Yucatan peninsula, southern Florida). Furthermore, the Loop Current, a major oceanic current, runs through the Gulf, variably interacting with the shelf. Thus, the Gulf of Mexico is a unique basin for the study of margin/open ocean interactions. Surprisingly, though, despite the significant interest in Louisiana Shelf hypoxia in the northern Gulf as well as recent studies engendered by the Deepwater Horizon blowout, few studies have addressed the issue of the shelf's influence on open Gulf waters and then generally only in a tangential way. For instance, early studies by Brooks et al. [104], Reid [105], and Todd et al. [106] all pointed to the likelihood of off-shelf transport of methane and radium in the Gulf. Likewise, Trefry and Presley [107] suggested that Mn fluxes from shelf sediments provided a source for 'excess' Mn in deep Gulf of Mexico sediments. Nonetheless, these studies have not been followed up by more detailed surveys or process studies. Surprisingly, TEI distributions in open waters of the Gulf are generally unknown.

In this report, we have summarized evidence supporting the importance of continental shelves and shelf seas in the oceanic mass balance of TEIs. Furthermore, we have outlined a methodology utilizing ^{228}Ra to more consistently estimate the flux of TEIs from the margins to the open ocean. To improve these estimates, we recommend that GEOTRACES sections place more emphasis on sampling along the margins and that increased consideration be given to completing margin-focused sections, such as that previously proposed for the Gulf of Mexico.

Data accessibility

<http://data.bco-dmo.org/jg/dir/BCO/GEOTRACES/NorthAtlanticTransect/>

Authors' contributions

All authors contributed to the discussion that formed the basis of this manuscript during the Royal Society workshop on “Quantifying fluxes and processes in trace-metal cycling at ocean boundaries” (Chicheley Hall, UK, December 9-10, 2015). M.A.C. wrote the manuscript with significant written contributions or editorial comments from all authors. M.A.C., P.J.L., M.C.L, and E.Y.K. developed the concept for ^{228}Ra as a TEI shelf flux gauge. V.H. and G.A.C. wrote the introduction. A.M. organized the vast reference list. C.J., A.M.S., P.W.B., W.B.H., H.T., P.S.A., D.P., and F.D. contributed written examples and figures for the review section of the manuscript. All authors gave final approval for publication.

Competing interests

The authors' declare no competing interests.

Funding

This paper would not have been possible without the financial support of a number of national funding agencies (U.S. NSF OCE-1458305 to M.A.C.; Korea NRF-2013R1A1A1058203 to E.Y.K; U.K. NERC NE/G016267/1 to M.C.L and A.M.; U.K. NERC NE/K009532/1 to W.B.H.).

Acknowledgements

We thank Gideon Henderson and the meeting organizers for inviting us to participate in the Royal Society workshop and contribute a paper to the special issue. For their constructive comments on the manuscript the authors thank Editor Micha Rijkenberg, Michiel Rutgers van der Loeff, and one anonymous reviewer. We gratefully acknowledge Francois Primeau for his feedback on derivation of the TEI flux model and Abby Bull of the British Oceanographic Data Centre for her assistance with data mining for the paper.

576

577 **Literature Cited**

- 578 1. Simpson JH, Sharples J. Introduction to the Physical and Biological
579 Oceanography of Shelf Seas: Cambridge University Press; 2012.
- 580 2. Bourgeois T, Orr JC, Resplandy L, Ethé C, Gehlen M, Bopp L. Coastal-ocean
581 uptake of anthropogenic carbon. *Biogeosci Disc.* 2016;2016:1-34.
- 582 3. Chen C-TA, Borges AV. Reconciling opposing views on carbon cycling in the
583 coastal ocean: Continental shelves as sinks and near-shore ecosystems as
584 sources of atmospheric CO₂. *Deep Sea Res (Part II: Top Stud Oceanogr).*
585 2009;56(8-10):578-90.
- 586 4. Regnier P, Friedlingstein P, Ciais P, Mackenzie FT, Gruber N, Janssens IA, et al.
587 Anthropogenic perturbation of the carbon fluxes from land to ocean. *Nature*
588 *Geo.* 2013;6(8):597-607.
- 589 5. Olausson E, Cato I, (Eds). Chemistry and biochemistry of estuaries.
590 Chichester: John Wiley & Sons Ltd; 1980. 452 p.
- 591 6. Boyle EA, Edmond JM, Sholkovitz ER. Mechanism of iron removal in
592 estuaries. *Geochim Cosmochim Acta.* 1977;41(9):1313-24.
- 593 7. Eckert JM, Sholkovitz ER. Flocculation of iron, aluminum and humates from
594 river water by electrolytes. *Geochim Cosmochim Acta.* 1976;40(7):847-8.
- 595 8. Sholkovitz ER, Copland D. The coagulation, solubility and adsorption
596 properties of Fe, Mn, Cu, Ni, Cd, Co and humic acids in a river water. *Geochim*
597 *Cosmochim Acta.* 1981;45(2):181-9.
- 598 9. Barnes CE, Cochran JK. Uranium geochemistry in estuarine sediments -
599 controls on removal and release processes. *Geochim Cosmochim Acta.*
600 1993;57(3):555-69.
- 601 10. Church TM, Sarin MM, Fleisher MQ, Ferdelman TG. Salt marshes: An
602 important coastal sink for dissolved uranium. *Geochim Cosmochim Acta.*
603 1996;60(20):3879-87.
- 604 11. Andersen MB, Stirling CH, Porcelli D, Halliday AN, Andersson PS, Baskaran M.
605 The tracing of riverine U in Arctic seawater with very precise U-234/U-238
606 measurements. *Earth Planet Sci Lett.* 2007;259(1-2):171-85.
- 607 12. Elderfield H, Upstillgoddard R, Sholkovitz ER. The rare-earth elements in
608 rivers, estuaries, and coastal seas and their significance to the composition of
609 ocean waters. *Geochim Cosmochim Acta.* 1990;54(4):971-91.
- 610 13. Rousseau TCC, Sonke JE, Chmeleff J, van Beek P, Souhaut M, Boaventura G, et
611 al. Rapid neodymium release to marine waters from lithogenic sediments in
612 the Amazon estuary. *Nature Comm.* 2015;6.
- 613 14. Sholkovitz E, Szymczak R. The estuarine chemistry of rare earth elements:
614 comparison of the Amazon, Fly, Sepik and the Gulf of Papua systems. *Earth*
615 *Planet Sci Lett.* 2000;179(2):299-309.
- 616 15. Sholkovitz ER, Cochran JK, Carey AE. Laboratory studies of the diagenesis
617 and mobility of Pu-239, Pu-240 and Cs-137 in nearshore sediments. *Geochim*
618 *Cosmochim Acta.* 1983;47(8):1369-79.

- 619 16. Carroll J, Falkner KK, Brown ET, Moore WS. The role of the Ganges-
620 Brahmaputra mixing zone in supplying barium and Ra-226 to the Bay of
621 Bengal. *Geochim Cosmochim Acta*. 1993;57(13):2981-90.
- 622 17. Coffey M, Dehairs F, Collette O, Luther G, Church T, Jickells T. The behaviour
623 of dissolved barium in estuaries. *Estuar Coast Shelf Sci*. 1997;45(1):113-21.
- 624 18. Edmond JM, Boyle ED, Drummond D, Grant B, Mislick T. Desorption of
625 barium in the plume of the Zaire (Congo) River. *Netherlands J of Sea Res*.
626 1978;12(3-4):324-8.
- 627 19. Hanor JS, Chan LH. Non-conservative behaviour of barium during mixing of
628 Mississippi River and Gulf of Mexico waters. *Earth Planet Sci Lett*.
629 1977;37(2):242-50.
- 630 20. Li YH, Chan LH. Desorption of Ba and Ra-226 from river-borne sediments in
631 the Hudson estuary. *Earth Planet Sci Lett*. 1979;43(3):343-50.
- 632 21. Martin JM, Meybeck M. Elemental mass-balance of material carried by major
633 world rivers. *Mar Chem*. 1979;7(3):173-206.
- 634 22. Burnett WC, Dulaiova H, Stringer C, Peterson R. Submarine groundwater
635 discharge: Its measurement and influence on the coastal zone. *J Coast Res*.
636 2006;35-8.
- 637 23. Moore WS. Large groundwater inputs to coastal waters revealed by Ra-226
638 enrichments. *Nature*. 1996;380(6575):612-4.
- 639 24. Moore WS, Sarmiento JL, Key RM. Submarine groundwater discharge
640 revealed by Ra-228 distribution in the upper Atlantic Ocean. *Nature Geo*.
641 2008;1(5):309-11.
- 642 25. Rodellas V, Garcia-Orellana J, Masque P, Feldman M, Weinstein Y. Submarine
643 groundwater discharge as a major source of nutrients to the Mediterranean
644 Sea. *Proc Natl Acad Sci USA*. 2015;112(13):3926-30.
- 645 26. Kwon EY, Kim G, Primeau F, Moore WS, Cho H-M, DeVries T, et al. Global
646 estimate of submarine groundwater discharge based on an observationally
647 constrained radium isotope model. *Geophys Res Lett*. 2014;41(23):8438-44.
- 648 27. Windom HL, Moore WS, Niencheski LFH, Jahrike RA. Submarine groundwater
649 discharge: A large, previously unrecognized source of dissolved iron to the
650 South Atlantic Ocean. *Mar Chem*. 2006;102(3-4):252-66.
- 651 28. Bone SE, Charette MA, Lamborg CH, Gonneea ME. Has submarine
652 groundwater discharge been overlooked as a source of mercury to coastal
653 waters? *Environ Sci Technol*. 2007;41(9):3090-5.
- 654 29. Trezzi G, Garcia-Orellana J, Santos-Echeandia J, Rodellas V, Garcia-Solsona E,
655 Garcia-Fernandez G, et al. The influence of a metal-enriched mining waste
656 deposit on submarine groundwater discharge to the coastal sea. *Mar Chem*.
657 2016;178:35-45.
- 658 30. Gonneea ME, Charette MA, Liu Q, Herrera-Silveira JA, Morales-Ojeda SM.
659 Trace element geochemistry of groundwater in a karst subterranean estuary
660 (Yucatan Peninsula, Mexico). *Geochim Cosmochim Acta*. 2014;132:31-49.
- 661 31. Arsouze T, Dutay JC, Lacan F, Jeandel C. Reconstructing the Nd oceanic cycle
662 using a coupled dynamical - biogeochemical model. *Biogeosciences*.
663 2009;6(12):2829-46.

- 664 32. Jeandel C, Oelkers EH. The influence of terrigenous particulate material
665 dissolution on ocean chemistry and global element cycles. *Chem Geol.*
666 2015;395:50-66.
- 667 33. Tachikawa K, Athias V, Jeandel C. Neodymium budget in the modern ocean
668 and paleo-oceanographic implications. *J Geophys Res:Oceans.* 2003;108(C8).
- 669 34. Abbott AN, Haley BA, McManus J, Reimers CE. The sedimentary flux of
670 dissolved rare earth elements to the ocean. *Geochim Cosmochim Acta.*
671 2015;154:186-200.
- 672 35. Blain S, Queguiner B, Armand L, Belviso S, Bombled B, Bopp L, et al. Effect of
673 natural iron fertilization on carbon sequestration in the Southern Ocean.
674 *Nature.* 2007;446(7139):1070-U1.
- 675 36. Bowie AR, van der Merwe P, Queroue F, Trull T, Fourquez M, Planchon F, et
676 al. Iron budgets for three distinct biogeochemical sites around the Kerguelen
677 Archipelago (Southern Ocean) during the natural fertilisation study, KEOPS-
678 2. *Biogeosciences.* 2015;12(14):4421-45.
- 679 37. Pollard RT, Salter I, Sanders RJ, Lucas MI, Moore CM, Mills RA, et al. Southern
680 Ocean deep-water carbon export enhanced by natural iron fertilization.
681 *Nature.* 2009;457(7229):577-U81.
- 682 38. Anderson RF, Mawji E, Cutter GA, Measures CI, Jeandel C. GEOTRACES
683 Changing the Way We Explore Ocean Chemistry. *Oceanography.*
684 2014;27(1):50-61.
- 685 39. Anderson RF, Henderson GM. Program update: GEOTRACES—A Global study
686 of the marine biogeochemical cycles of trace elements and their isotopes.
687 *Oceanography.* 2005;18(3):76-9.
- 688 40. Plan GS. GEOTRACES: An international study of the marine biogeochemical
689 cycles of traces elements and their isotopes: Scientific Committee in Ocean
690 Research; 2006.
- 691 41. Mawji E, Schlitzer R, Dodas EM, Abadie C, Abouchami W, Anderson RF, et al.
692 The GEOTRACES Intermediate Data Product 2014. *Mar Chem.* 2015;177:1-8.
- 693 42. Glavovic BC, Limburg K, Liu KK, Emeis KC, Thomas H, Kremer H, et al. Living
694 on the Margin in the Anthropocene: engagement arenas for sustainability
695 research and action at the ocean-land interface. *Curr Opin Env Sustain.*
696 2015;14:232-8.
- 697 43. McGranahan G, Balk D, Anderson B. The rising tide: assessing the risks of
698 climate change and human settlements in low elevation coastal zones.
699 *Environ Urban.* 2007;19(1):17-37.
- 700 44. Small C, Nicholls RJ. A global analysis of human settlement in coastal zones. *J*
701 *Coast Res.* 2003;19(3):584-99.
- 702 45. Boyle EA, Lee J-M, Echegoyen Y, Noble A, Moos S, Carrasco G, et al.
703 Anthropogenic Lead Emission in the Ocean The Evolving Global Experiment.
704 *Oceanography.* 2014;27(1):69-75.
- 705 46. Lamborg CH, Hammerschmidt CR, Bowman KL, Swarr GJ, Munson KM,
706 Ohnemus DC, et al. A global ocean inventory of anthropogenic mercury based
707 on water column measurements. *Nature.* 2014;512(7512):65-+.

- 708 47. Bhatia MP, Kujawinski EB, Das SB, Breier CF, Henderson PB, Charette MA.
709 Greenland meltwater as a significant and potentially bioavailable source of
710 iron to the ocean. *Nature Geo.* 2013;6(4):274-8.
- 711 48. Hopwood MJ, Bacon S, Arendt K, Connelly DP, Statham PJ. Glacial meltwater
712 from Greenland is not likely to be an important source of Fe to the North
713 Atlantic. *Biogeochemistry.* 2015;124(1-3):1-11.
- 714 49. Jeandel C. Solid river inputs and ocean margins as critical sources of elements
715 to the oceans. *Philos Trans R Soc London, Ser A.* 2016;In Press (this issue).
- 716 50. Jakobsson M. Hypsometry and volume of the Arctic Ocean and its constituent
717 seas. *Geochim Geophys Geosystems.* 2002;3.
- 718 51. Aagaard K, Carmack EC. The role of sea ice and other freshwater in the arctic
719 circulation. *J Geophys Res:Oceans.* 1989;94(C10):14485-98.
- 720 52. Moore RM. Oceanographic distributions of zinc, cadmium, copper and
721 aluminum in waters of the central Arctic. *Geochim Cosmochim Acta.*
722 1981;45(12):2475-82.
- 723 53. Ripperger S, Rehkaemper M, Porcelli D, Halliday AN. Cadmium isotope
724 fractionation in seawater - A signature of biological activity. *Earth Planet Sci*
725 *Lett.* 2007;261(3-4):670-84.
- 726 54. Lambelet M, Rehkaemper M, de Fliedrt Tv, Xue Z, Kreissig K, Coles B, et al.
727 Isotopic analysis of Cd in the mixing zone of Siberian rivers with the Arctic
728 Ocean-New constraints on marine Cd cycling and the isotope composition of
729 riverine Cd. *Earth Planet Sci Lett.* 2013;361:64-73.
- 730 55. Roeske T, Bauch D, Van Der Loeff MR, Rabe B. Utility of dissolved barium in
731 distinguishing North American from Eurasian runoff in the Arctic Ocean. *Mar*
732 *Chem.* 2012;132:1-14.
- 733 56. Thomas H, Shadwick E, Dehairs F, Lansard B, Mucci A, Navez J, et al. Barium
734 and carbon fluxes in the Canadian Arctic Archipelago. *J Geophys Res:Oceans.*
735 2011;116.
- 736 57. Middag R, de Baar HJW, Laan P, Klunder MB. Fluvial and hydrothermal input
737 of manganese into the Arctic Ocean. *Geochim Cosmochim Acta.*
738 2011;75(9):2393-408.
- 739 58. McAlister JA, Orians KJ. Dissolved gallium in the Beaufort Sea of the Western
740 Arctic Ocean: A GEOTRACES cruise in the International Polar Year. *Mar*
741 *Chem.* 2015;177:101-9.
- 742 59. Andersson PS, Porcelli D, Frank M, Bjork G, Dahlqvist R, Gustafsson O.
743 Neodymium isotopes in seawater from the Barents Sea and Fram Strait
744 Arctic-Atlantic gateways. *Geochim Cosmochim Acta.* 2008;72(12):2854-67.
- 745 60. Porcelli D, Andersson PS, Baskaran M, Frank M, Bjork G, Semiletov I. The
746 distribution of neodymium isotopes in Arctic Ocean basins. *Geochim*
747 *Cosmochim Acta.* 2009;73(9):2645-59.
- 748 61. Dahlqvist RM, Andersson PS, Porcelli D. REE seawater concentrations in the
749 Bering Strait and the Chukchi Sea. *Ocean Sciences 2008 Meeting Poster*
750 *session #0722008.*
- 751 62. Persson P, Andersson PS, Porcelli D, Semiletov I. The influence of Lena River
752 water inflow and shelf sediment-sea water exchange for the Nd isotopic

composition in the Laptev Sea and Arctic Ocean. European Geosciences Union 2011 Meeting Abstract 1012032011.

63. Alling V, Sanchez-Garcia L, Porcelli D, Pugach S, Vonk JE, van Dongen B, et al. Nonconservative behavior of dissolved organic carbon across the Laptev and East Siberian seas. *Global Biogeochem Cycles*. 2010;24.

64. Alling V, Porcelli D, Morth CM, Anderson LG, Sanchez-Garcia L, Gustafsson O, et al. Degradation of terrestrial organic carbon, primary production and outgassing of CO₂ in the Laptev and East Siberian Seas as inferred from delta C-13 values of DIC. *Geochim Cosmochim Acta*. 2012;95:143-59.

65. Portnov A, Smith AJ, Mienert J, Cherkashov G, Rekant P, Semenov P, et al. Offshore permafrost decay and massive seabed methane escape in water depths > 20m at the South Kara Sea shelf. *Geophys Res Lett*. 2013;40(15):3962-7.

66. Shakhova N, Semiletov I, Salyuk A, Yusupov V, Kosmach D, Gustafsson O. Extensive Methane Venting to the Atmosphere from Sediments of the East Siberian Arctic Shelf. *Science*. 2010;327(5970):1246-50.

67. Whitmore L, Shiller AM. Dissolved methane in the US GEOTRACES Arctic section. *Ocean Sciences 2016 Meeting Poster A44A-26832016*.

68. Rutgers van der Loeff M, Key RM, Scholten J, Bauch D, Michel A. Ra-228 as a tracer for shelf water in the Arctic Ocean. *Deep Sea Res (Part II: Top Stud Oceanogr)*. 1995;42(6):1533-53.

69. Rutgers van der Loeff M, Cai P, Stimac I, Bauch D, Hanfland C, Roeske T, et al. Shelf-basin exchange times of Arctic surface waters estimated from Th-228/Ra-228 disequilibrium. *J Geophys Res:Oceans*. 2012;117.

70. Aguilar-Islas AM, Hurst MP, Buck KN, Sohst B, Smith GJ, Lohan MC, et al. Micro- and macronutrients in the southeastern Bering Sea: Insight into iron-replete and iron-depleted regimes. *Prog Oceanogr*. 2007;73(2):99-126.

71. Elrod VA, Berelson WM, Coale KH, Johnson KS. The flux of iron from continental shelf sediments: A missing source for global budgets. *Geophys Res Lett*. 2004;31(12):art. no.-L12307.

72. Tyrrell T, Merico A, Waniek JJ, Wong CS, Metzl N, Whitney F. Effect of seafloor depth on phytoplankton blooms in high-nitrate, low-chlorophyll (HNLC) regions. *J Geophys Res: Biogeosci*. 2005;110(G2).

73. Tagliabue A, Aumont O, Bopp L. The impact of different external sources of iron on the global carbon cycle. *Geophys Res Lett*. 2014;41(3):920-6.

74. Charette MA, Gonneea ME, Morris PJ, Statham P, Fones G, Planquette H, et al. Radium isotopes as tracers of iron sources fueling a Southern Ocean phytoplankton bloom. *Deep Sea Res (Part II: Top Stud Oceanogr)*. 2007;54(18-20):1989-98.

75. Dulaiova H, Ardelan MV, Henderson PB, Charette MA. Shelf-derived iron inputs drive biological productivity in the southern Drake Passage. *Global Biogeochem Cycles*. 2009;23.

76. van Beek P, Bourquin M, Reyss JL, Souhaut M, Charette MA, Jeandel C. Radium isotopes to investigate the water mass pathways on the Kerguelen Plateau (Southern Ocean). *Deep Sea Res (Part II: Top Stud Oceanogr)*. 2008;55(5-7):622-37.

77. Boyd PW, Strzepek R, Chiswell S, Chang H, DeBruyn JM, Ellwood M, et al. Microbial control of diatom bloom dynamics in the open ocean. *Geophys Res Lett*. 2012;39.
78. John SG, Adkins J. The vertical distribution of iron stable isotopes in the North Atlantic near Bermuda. *Global Biogeochem Cycles*. 2012;26.
79. Labatut M, Lacan F, Pradoux C, Chmeleff J, Radic A, Murray JW, et al. Iron sources and dissolved-particulate interactions in the seawater of the Western Equatorial Pacific, iron isotope perspectives. *Global Biogeochem Cycles*. 2014;28(10):1044-65.
80. Lacan F, Radic A, Jeandel C, Poitrasson F, Sarthou G, Pradoux C, et al. Measurement of the isotopic composition of dissolved iron in the open ocean. *Geophys Res Lett*. 2008;35(24):5.
81. Radic A, Lacan F, Murray JW. Iron isotopes in the seawater of the equatorial Pacific Ocean: New constraints for the oceanic iron cycle. *Earth Planet Sci Lett*. 2011;306(1-2):1-10.
82. Conway TM, Rosenberg AD, Adkins JF, John SG. A new method for precise determination of iron, zinc and cadmium stable isotope ratios in seawater by double-spike mass spectrometry. *Anal Chim Acta*. 2013;793:44-52.
83. Conway TM, John SG. Quantification of dissolved iron sources to the North Atlantic Ocean. *Nature*. 2014;511(7508):212-+.
84. Fitzsimmons JN, Carrasco GG, Wu J, Roshan S, Hatta M, Measures CI, et al. Partitioning of dissolved iron and iron isotopes into soluble and colloidal phases along the GA03 GEOTRACES North Atlantic Transect. *Deep Sea Res (Part II: Top Stud Oceanogr)*. 2015;116:130-51.
85. Homoky WB, John SG, Conway TM, Mills RA. Distinct iron isotopic signatures and supply from marine sediment dissolution. *Nature Comm*. 2013;4:10.
86. Homoky WB, Severmann S, Mills RA, Statham PJ, Fones GR. Pore-fluid Fe isotopes reflect the extent of benthic Fe redox recycling: Evidence from continental shelf and deep-sea sediments. *Geology*. 2009;37(8):751-4.
87. Homoky WB, Hembury DJ, Hepburn LE, Mills RA, Statham PJ, Fones GR, et al. Iron and manganese diagenesis in deep sea volcanogenic sediments and the origins of pore water colloids. *Geochim Cosmochim Acta*. 2011;75(17):5032-48.
88. Homoky WB, Weber T, Berelson WM, Conway TM, Henderson GM, van Hulten M, et al. An assessment of oceanic trace element and isotope exchange at the sediment-water boundary. *Philos Trans R Soc London, Ser A*. 2016;In Press (this issue).
89. Charette MA, Morris PJ, Henderson PB, Moore WS. Radium isotope distributions during the US GEOTRACES North Atlantic cruises. *Mar Chem*. 2015;177:184-95.
90. Moore WS, Astwood H, Lindstrom C. Radium isotopes in coastal waters on the Amazon shelf. *Geochim Cosmochim Acta*. 1995;59(20):4285-98.
91. Krest JM, Moore WS, Rama. Ra-226 and Ra-228 in the mixing zones of the Mississippi and Atchafalaya Rivers: indicators of groundwater input. *Mar Chem*. 1999;64(3):129-52.

- 844 92. Moore WS. Inappropriate attempts to use distributions of Ra-228 and Ra-226
845 in coastal waters to model mixing and advection rates. *Cont Shelf Res.*
846 2015;105:95-100.
- 847 93. Moore WS. Determining coastal mixing rates using radium isotopes. *Cont*
848 *Shelf Res.* 2000;20(15):1993-2007.
- 849 94. Saito MA, Moffett JW, DiTullio GR. Cobalt and nickel in the Peru upwelling
850 region: A major flux of labile cobalt utilized as a micronutrient. *Global*
851 *Biogeochem Cycles.* 2004;18(4).
- 852 95. Bown J, Boye M, Baker A, Duvieilbourg E, Lacan F, Le Moigne F, et al. The
853 biogeochemical cycle of dissolved cobalt in the Atlantic and the Southern
854 Ocean south off the coast of South Africa. *Mar Chem.* 2011;126(1-4):193-206.
- 855 96. Dale AW, Nickelsen L, Scholz F, Hensen C, Oschlies A, Wallmann K. A revised
856 global estimate of dissolved iron fluxes from marine sediments. *Global*
857 *Biogeochem Cycles.* 2015;29(5):691-707.
- 858 97. Landing WM, Bruland KW. The Contrasting Biogeochemistry of Iron and
859 Manganese in the Pacific-Ocean. *Geochim Cosmochim Acta.* 1987;51(1):29-
860 43.
- 861 98. McManus J, Berelson WM, Severmann S, Johnson KS, Hammond DE, Roy M, et
862 al. Benthic manganese fluxes along the Oregon-California continental shelf
863 and slope. *Cont Shelf Res.* 2012;43:71-85.
- 864 99. Saito MA, Moffett JW. Temporal and spatial variability of cobalt in the Atlantic
865 Ocean. *Geochim Cosmochim Acta.* 2002;66(11):1943-53.
- 866 100. Dulaquais G, Boye M, Rijkenberg MJA, Carton X. Physical and
867 remineralization processes govern the cobalt distribution in the deep
868 western Atlantic Ocean. *Biogeosciences.* 2014;11(6):1561-80.
- 869 101. Powell CF, Baker AR, Jickells TD, Bange HW, Chance RJ, Yodle C. Estimation of
870 the Atmospheric Flux of Nutrients and Trace Metals to the Eastern Tropical
871 North Atlantic Ocean. *J Atmos Sci.* 2015;72(10):4029-45.
- 872 102. Little SH, Vance D, Walker-Brown C, Landing WM. The oceanic mass balance
873 of copper and zinc isotopes, investigated by analysis of their inputs, and
874 outputs to ferromanganese oxide sediments. *Geochim Cosmochim Acta.*
875 2014;125:673-93.
- 876 103. Tanaka T, Yasuda I, Kuma K, Nishioka J. Vertical turbulent iron flux sustains
877 the Green Belt along the shelf break in the southeastern Bering Sea. *Geophys*
878 *Res Lett.* 2012;39.
- 879 104. Brooks JM, Reid DF, Bernard BB. Methane in the upper water column of the
880 northwestern Gulf of Mexico. *J Geophys Res:Oceans.* 1981;86(NC11):1029-
881 40.
- 882 105. Reid DF. Radium variability produced by shelf-water transport and mixing in
883 the western Gulf of Mexico. *Deep Sea Res (Part I: Oceanogr Res Papers).*
884 1984;31(12):1501-10.
- 885 106. Todd JF, Wong GTF, Reid DF. The geochemistries of Po-210 and Pb-210 in
886 waters overlying and within the Orca Basin, Gulf of Mexico. *Deep Sea Res*
887 *(Part I: Oceanogr Res Papers).* 1986;33(10):1293-306.
- 888 107. Trefry JH, Presley BJ. Manganese fluxes from Mississippi Delta sediments.
889 *Geochim Cosmochim Acta.* 1982;46(10):1715-26.

890 108. Sholkovitz ER. The geochemistry of rare-earth elements in the Amazon River
891 estuary. *Geochim Cosmochim Acta*. 1993;57(10):2181-90.
892

Tables

Table 1. Western North Atlantic Ocean margin TEI flux estimates derived from shelf ²²⁸Ra inputs ($14.3 \pm 1.9 \times 10^{22}$ atoms/y; 0-70°N) and $\Delta\text{TEI}/\Delta^{228}\text{Ra}$ ratios. The integrated shelf area used to normalize the basin-scale fluxes was 2.5×10^{12} m².

	dCo	dFe	dMn	dZn
TEI/ ²²⁸ Ra ($\times 10^{-6}$ nmol/atom)	1.0	2.7	3.8	11
TEI Flux ($\times 10^8$ mol/y)	1.4	3.9	5.4	16
TEI Flux ($\mu\text{mol}/\text{m}^2/\text{y}$)	56	160	220	630

Figures

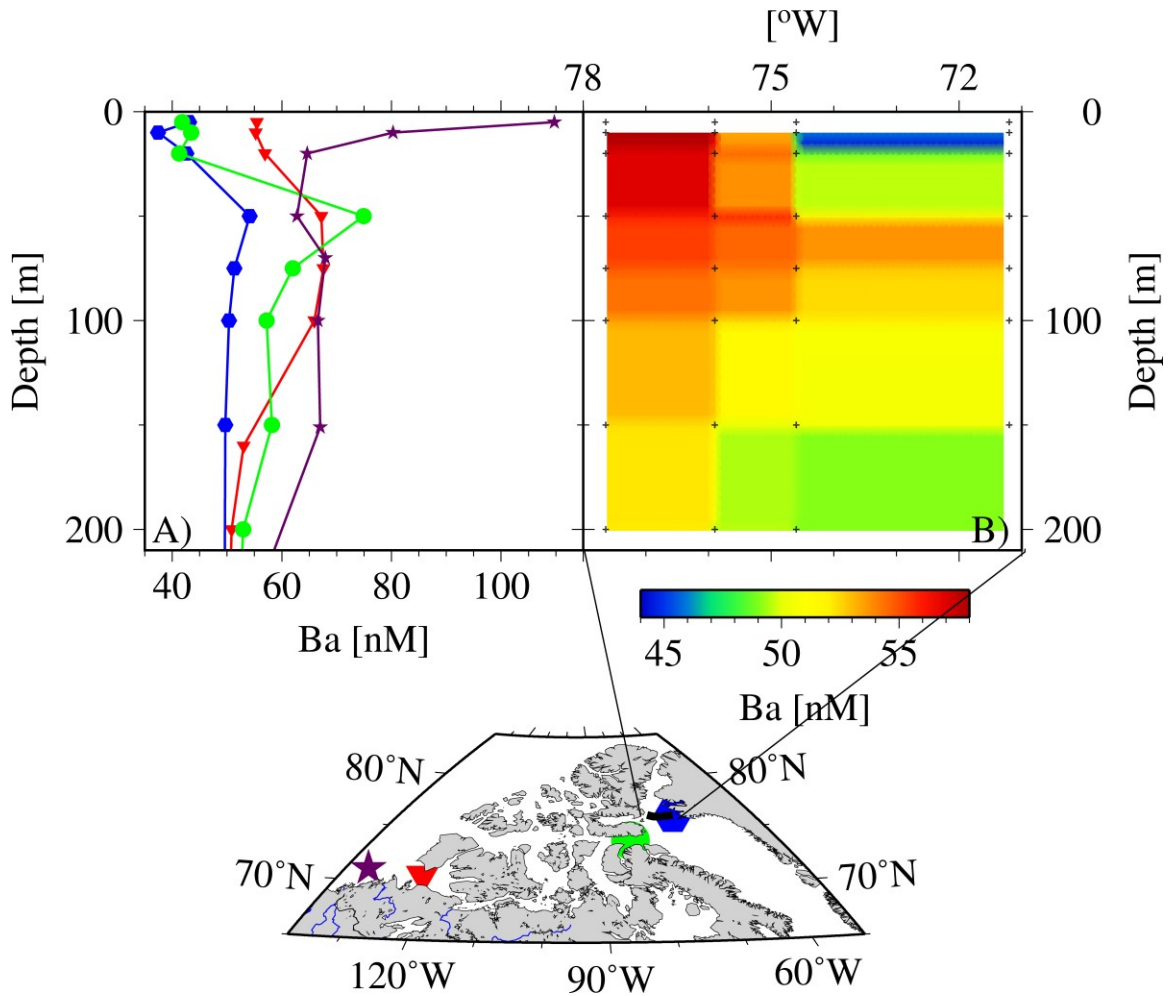


Figure 1. Dissolved Ba concentrations observed in the Canadian Arctic Archipelago during the Canadian CFL-IPY-GEOTRACES program in 2007-2008. A) Profiles of four selected stations across the Archipelago. The easternmost station (blue symbols) is under the influence of northward flowing North Atlantic waters, which reveal substantially lower Ba concentrations than waters sampled at stations within the Archipelago. The westernmost station (purple stars) near the Horton River estuary depicts the riverine surface source of Ba. In Archipelagic waters (green circles), Ba displays a subsurface maximum, which in turn can be used to trace the eastward transport of waters through the Archipelago (redrawn after Thomas et al. [56]). B) Ba contour section across the head of Baffin Bay, approximately along 76° N, as indicated by the black line in the inserted map in A). The easternmost station is identical with the one shown in A) (blue symbols).

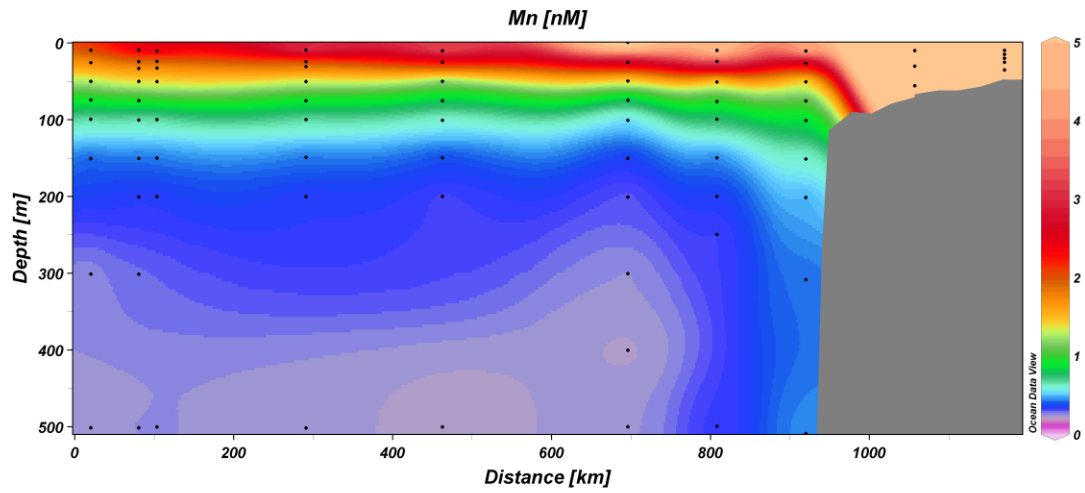
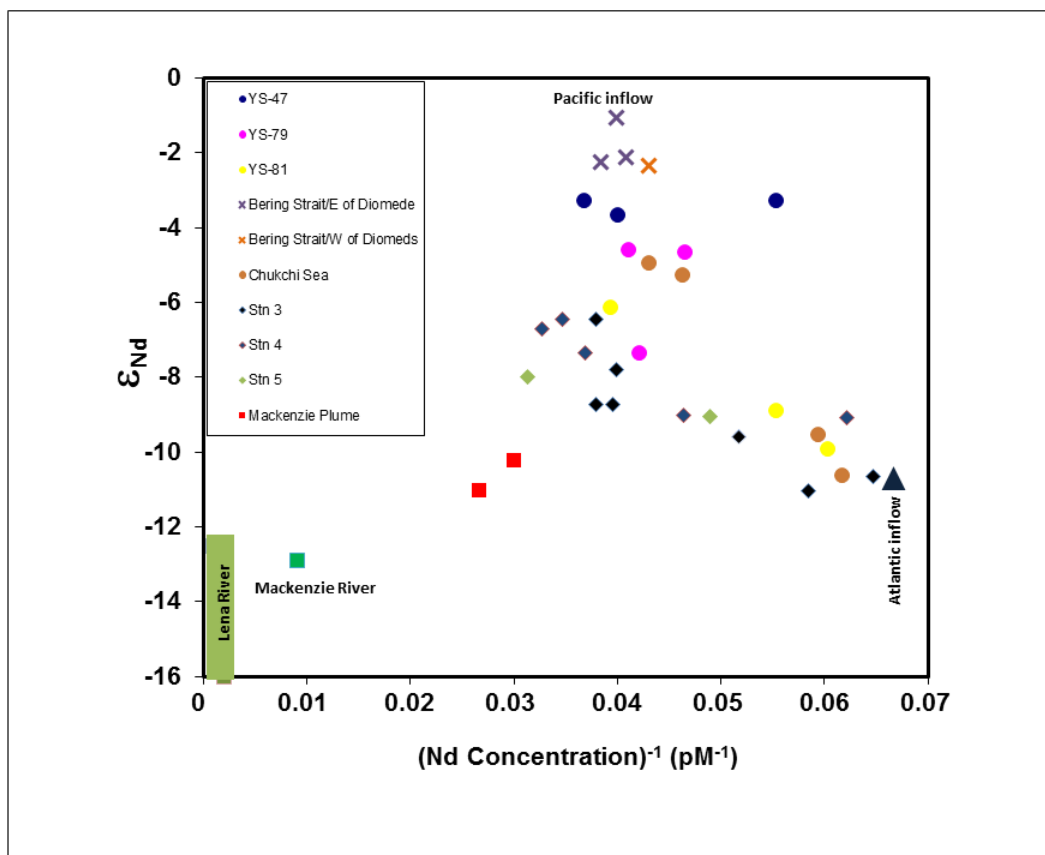


Figure 2. Dissolved Mn (nM) concentrations in the upper 500 m of the Laptev Sea illustrating the strong Mn source over the shelf and its subsequent transport toward the central Arctic basin (Middag et al. [57]).



920

921 Figure 3. Nd concentration and isotope data for Arctic Ocean waters. The isotope
 922 ratios of waters flowing from the Pacific decrease during passage through the
 923 Bering Sea before entering the Chukchi Sea in the Arctic due to interaction with
 924 shelf sediments (Dahlqvist et al. [61]).

925

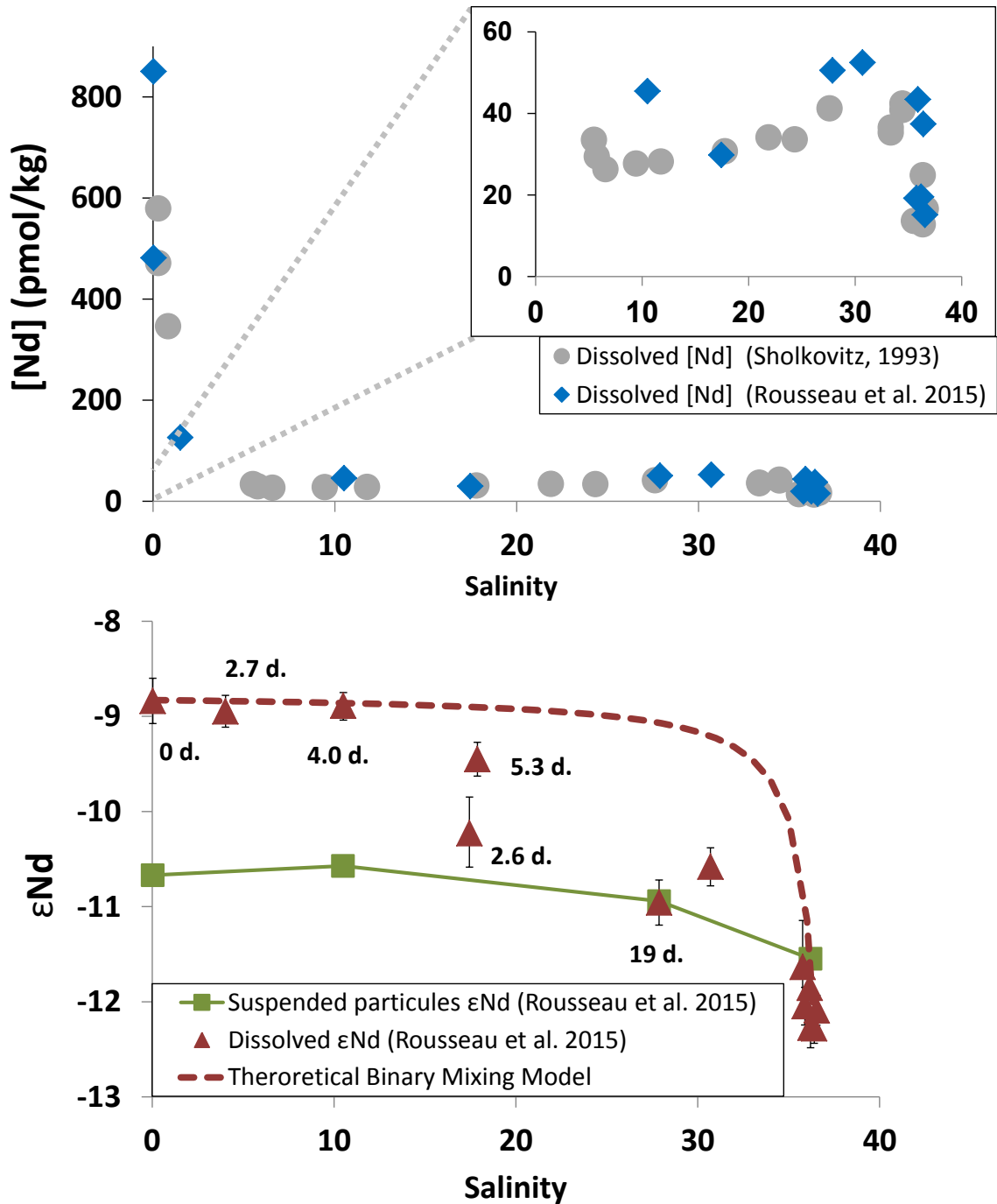


Figure 4. *Upper panel:* Amazon estuary [Nd] from Sholkovitz [108] (grey circles) and Rousseau et al. [13] (blue diamonds) are reported against the salinity gradient. *Lower panel:* Amazon estuary dissolved (red triangles), particulate (green squares) ϵNd and radium-derived water mass ages (in days) are reported against the salinity gradient.

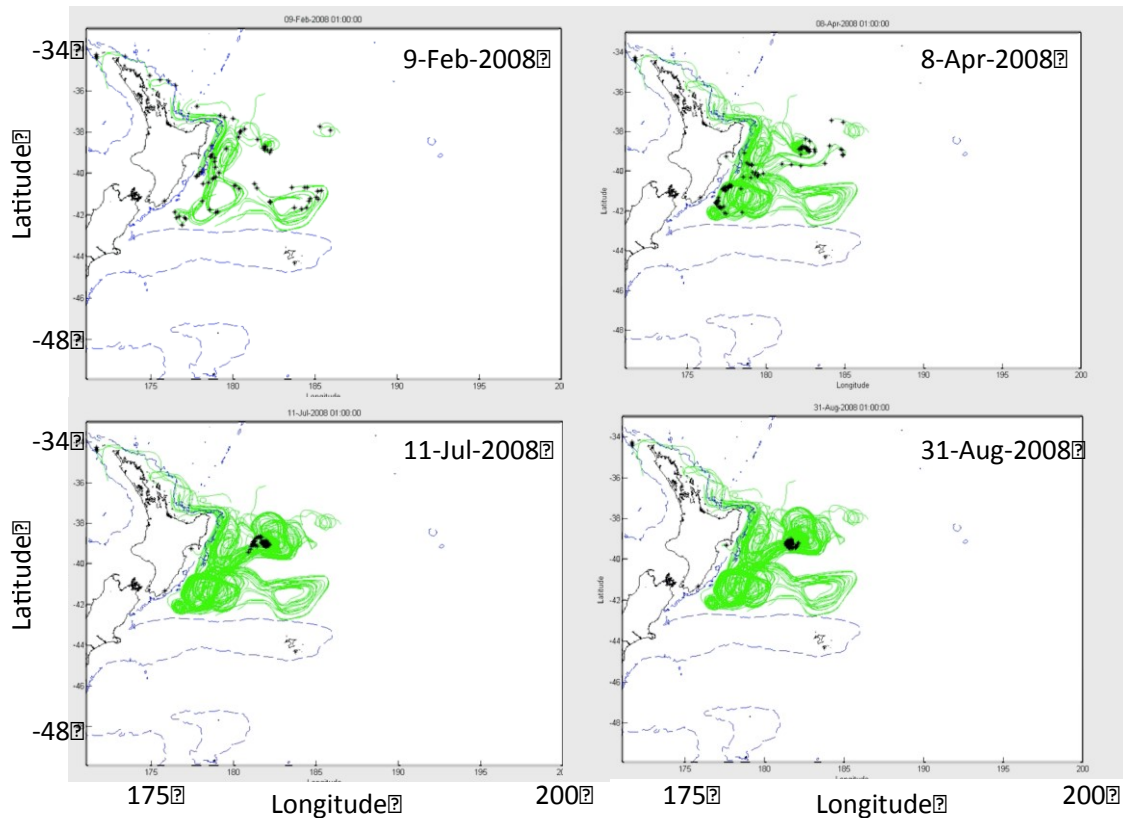


Figure 5. Particle trajectories (green lines) from an altimetry model designed to investigate the origin of water masses within a counterclockwise eddy studied as part of the GEOTRACES FeCycle process study (Boyd et al. [77]). Model snapshots are from (clockwise starting at top left) 9 Feb, 8 April, 11 July and 31 Aug 2008. The particles (black) traverse the waters on and across the 200 m deep shelf break (blue contours) adjacent to the eastern seaboard of the northern island of New Zealand.

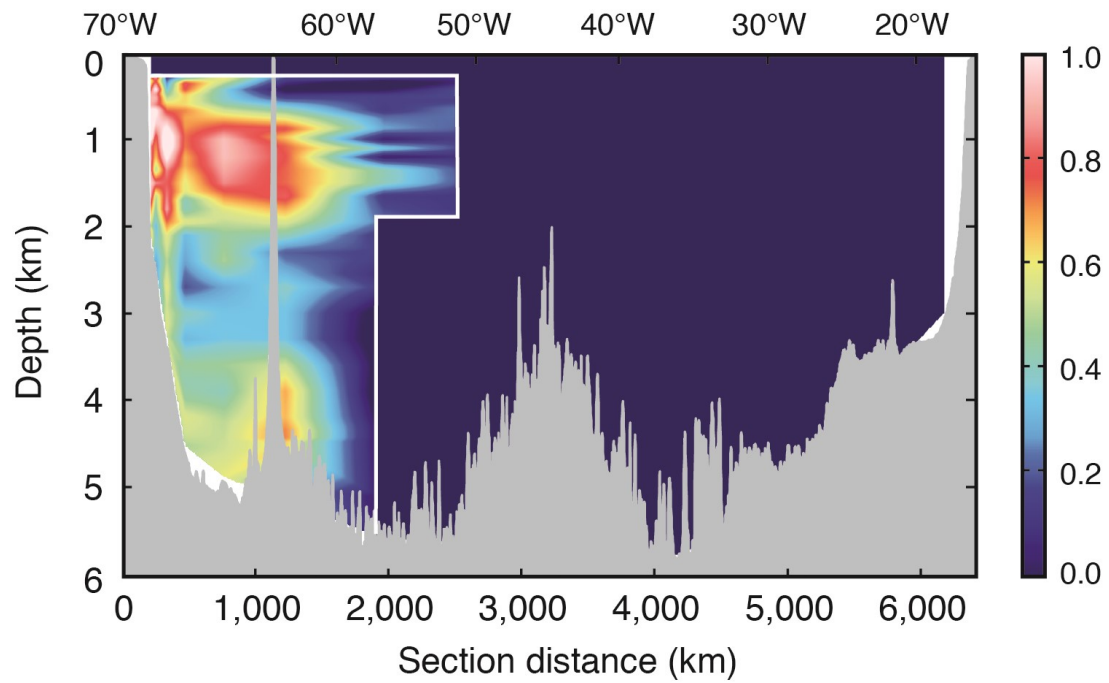


Figure 6. Fraction of water column Fe associated with input from oxygenated sediments along the North Atlantic margin (from Conway and John [83]).

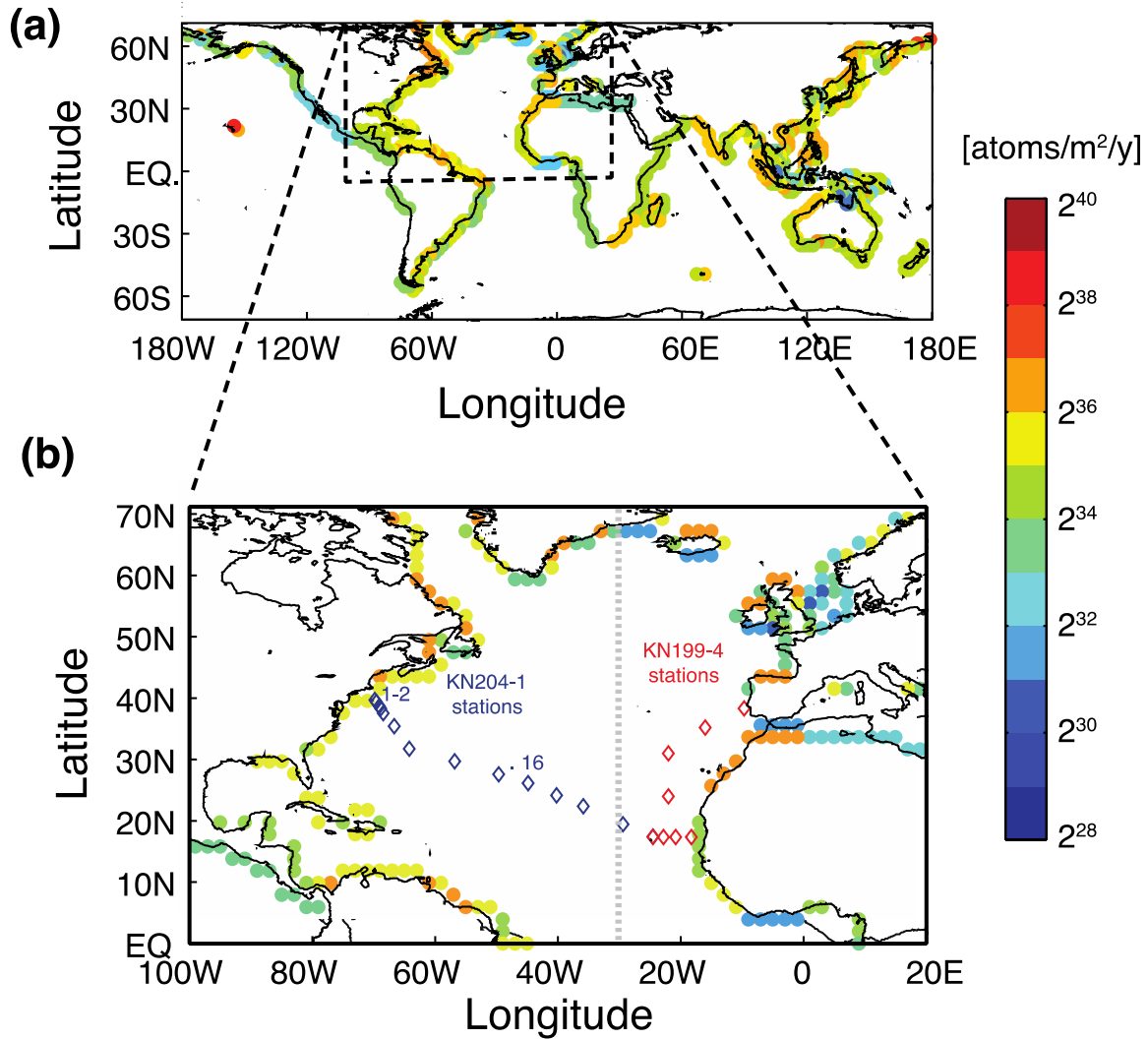


Figure 7. Model derived shelf ^{228}Ra flux (units are log base (2) atoms $\text{m}^{-2} \text{y}^{-1}$) from the model of Kwon et al. [26]. Also shown in (b) are the U.S. GEOTRACES GA03 cruise stations (diamonds). The dashed line in (b) is the boundary between the eastern and western Atlantic margins. The innermost coastal and central Atlantic stations were used to derive the $\Delta\text{TEI}/\Delta^{228}\text{Ra}$ averages.